Adaptive Redistributed Spatial Grids and Finite Volume Schemes for Hyperbolic Conservation Laws

Technical Report · October 2007

DOI: 10.13140/RG.2.2.19749.70883

2 authors, including:

Argiris Delis

Technical University of Crete

Adaptive Redistributed Spatial Grids and Finite Volume Schemes for Hyperbolic Conservation Laws

A.I. Delis[1] and Ch. Arvanitis[2]

[1] Department of Sciences-Division of Mathematics, Technical University of Crete, Chania, 73100, Greece adelis@science.tuc.gr
[2] Department of Mathematics & Statistics, University of Cyprus, 1678 Nicosia, Cyprus arvas@ucy.ac.cy

Summary. We study whether a dynamic mesh redistribution is a satisfactory mechanism for increasing the resolution of numerical solutions for problems of scalar and systems of conservation laws. Our redistribution policy is to reconstruct spatially the numerical solution on a new mesh, where the solution's curvature is almost uniformly distributed, while the nodes cardinality is kept constant. By adding this redistribution process as a sub-step on the time evolution step of some classical schemes with known (unstable) characteristics we conclude that the proposed redistribution adds stabilization properties while at the same time increases the resolution of the numerical schemes.

1 Introduction

Finite volume schemes is the common choice for computing solutions of systems of Conservation Laws in the context: *find* $u:\mathbb{R}^d \times [0,T] \rightarrow \mathbb{R}^M$ *such that*

$$\partial_t u + \sum_{i=1}^{d} \partial_{x_i} F_i(u) = 0, \quad u(\,\cdot, 0) = u_0 \ \textit{given.} \tag{1}$$

Classical schemes, of first or second order in space, when applied directly to this system will result to computational solutions with diffusive or oscillatory behavior, especially close to shocks. Mesh adaptation is a main current stream to efficiently compute numerical solutions of complex systems by increasing the resolution of the essential solution, see for example [TT]. In this work the evolving mesh is constructed such that its spatial resolution is controlled via selective characteristics of the computed solution. These characteristics are defined through a positive functional of the solution, the so called *estimator function* [AKM], [AMT], [ARV06]. Among other estimator functions for evolution PDE's, like the arc-length and variance, we choose the curvature of the solution as such function, for its diffuseless behavior. The adaptive grid redistribution procedure (**AGR**)studied in this work is based on a mesh redistribution policy that evolves within every computational time step. Our choice

of classical schemes include, for example, the first order Roe scheme, the second order Lax-Wendroff and MacCormack schemes and also some TVD schemes.

2 Adaptive Grid Redistribution (AGR)

We denote with X a partition of a computational domain $[a, b]$, with nodes $\{x_i\}_{i=0}^N$ and we introduce the notation:

- $\mathbf{resolution}(A) = \text{card}\{K \in X : K \subset A\}$,
- $\{u_i\}_{i=0}^N$ = vector of solution values on nodes of X, $U(X)$ piecewise constant function taking the value u_i on $[x_{i-1}^+, x_i^+)$, i.e.

$$U = \sum_{i=0}^{N} u_i \ \chi_{[x_{i-1}^+, x_i^+)} + u_N \ \chi_{\{x_N^+\}},$$

where $x_{-1}^+ = x_0, \ \ x_i^+ = x_{i+\frac{1}{2}}, i = 0, 1, \ldots, N-1, \ \ x_N^+ = x_N$.

The $\mathbf{AGR}$ procedure is then described by two sequential steps:

$$\tilde{X} = \mathbf{GMesh}(X, \ U(X)),$$
$$\tilde{U}(\tilde{X}) = \mathbf{Rec}(X, \ U(X), \ \tilde{X}).$$

2.1 The GMesh step

At this step of the $\mathbf{AGR}$ procedure, a new partition $\tilde{X}$ of spatial nodes $\{\tilde{x}_i\}_{i=0}^N$ is formed, with $\mathbf{resolution}$ controlled by selected characteristics of the numerical solution U. The step is accomplished in two phases schematically shown in Figs 1 and 2 on Reimann data.

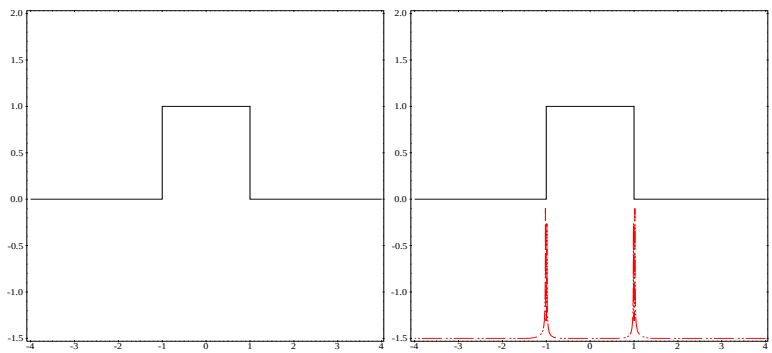

Fig. 1. Input data $X, U(X)$ (left) and Phase 1 (right)

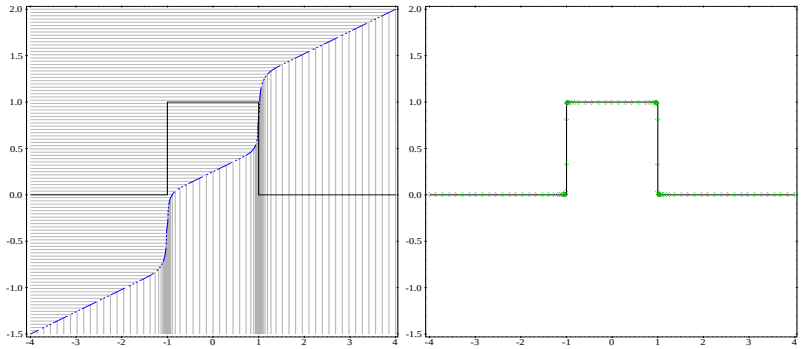

Fig. 2. Phase 2 (left) and Output data $\tilde{X}$, $\tilde{U}(\tilde{X})$ (right)

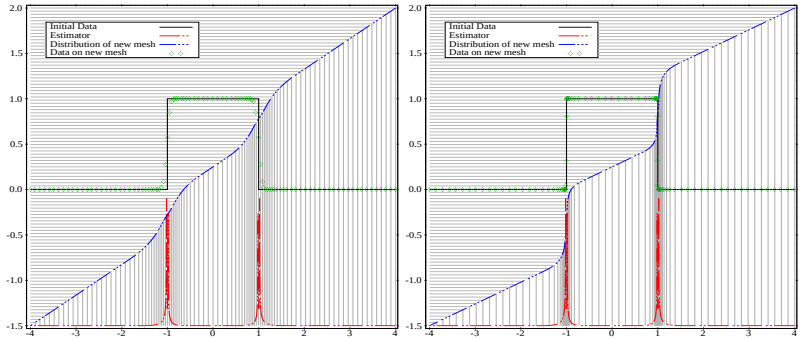

Fig. 3. The AGR for p=0.01 (left) and for p=0.05 (right)

Phase 1: creates the *estimator function*, in order to select the $\mathbf{resolution's}$ density of the new mesh. The value g_i, of the estimator function on the node x_i, is given by a power p of an approximation of the *curvature* of U,

$$g_i = \Big(2\frac{\|(A_{i+1}-A_i)\times(A_i-A_{i-1})\|}{\|A_{i+1}-A_i\|\,\|A_{i+1}-A_{i-1}\|\,\|A_i-A_{i-1}\|}\Big)^p,$$

where, the parameter $p \in [0,1]$ controls the upper bound of the new mesh density (an example of its action is shown in Fig. 3) and A_j denotes the plane point $(x_j, U(x_j))$.
Phase 2: defines the new mesh $\tilde{X}$ such that the measure $G_U(A) = \int_A (g_h \circ U)\, d\mu$ is equidisrtibuted on $\tilde{X}$, i.e.

$$\int_{\tilde{x}_{i-1}}^{\tilde{x}_i} g_h(U(x))\, dx = \frac{1}{N}\int_a^b g_h(U(x))\, dx, \quad i = 1,\ldots,N,$$

where $g_h \circ U$ is the piecewise constant function taking the value g_i on $[x_{i-1}^+, x_i^+)$. Then,

$$G_i = G_U([a, x_i]) = \int_{[a,x_i]} (g_h \circ U)\, d\mu = G_{i-1} + \int_{x_{i-1}}^{x_i} g_h(U(x))\, dx$$
$$= G_{i-1} + (g_{i-1} + g_i)(x_i - x_{i-1})/2$$

so, the nodes of the new mesh $\tilde{X}$ are given by,

$$\tilde{x}_i = x_{k_i} + \frac{x_{k_i+1} - x_{k_i}}{G_{k_i+1} - G_{k_i}}(\tilde{G}_i - G_{k_i}),$$

where $\tilde{G}_i = \frac{i}{N} G_N$, $k_i = \max_{k_{i-1} \le \ell \le N}\{\ell : G_\ell \le \tilde{G}_i\}$.

2.2 The Rec step.

The reconstructed solution $\tilde{U}$ is conservatively defined on each $[\tilde{x}^+_{i-1}, \tilde{x}^+_i]$ of the new mesh as,

$$\int_{\tilde{x}^+_{i-1}}^{\tilde{x}^+_i} \tilde{U}(x)\, dx = \int_{\tilde{x}^+_{i-1}}^{\tilde{x}^+_i} U(x)\, dx.$$

Thus, the values $\{\tilde{u}_i\}_{i=0}^N$ of the reconstructed solution on the new grid, are given by

$$\tilde{u}_i = \frac{(\tilde{x}^+_i - x^+_{k_i})u_{k_i+1} + \sum_{\ell=k_{i-1}+1}^{k_i}(x^+_\ell - x^+_{\ell-1})u_\ell - (\tilde{x}^+_{i-1} - x^+_{k_{i-1}})u_{k_{i-1}+1}}{\left(\tilde{x}^+_i - \tilde{x}^+_{i-1}\right)},$$

where $k_i = \max_{k_{i-1} \le \ell \le N}\{\ell : x^+_\ell \le \tilde{x}^+_i\}$.

A parameter D is also introduced such that $(\tilde{X}, \tilde{U}) = (X, U)$ when $|X - \tilde{X}| < D$, meaning that if the relative mean displacement between the current and the new mesh is small (to the order 10^{-2} and less) the procedure is avoided, see [ARV06] for details.

2.3 Implementation on Dynamic PDE's

Let $\mathbf{Solver}$ = a general finite volume scheme for non-uniform grids and, initial data U^0 defined on the uniform partition X^0 of $[a, b]$. Then we compute:

- Time evolution step on *uniform mesh*:
$$(X^n,\ U^n(X^n)) = (X^{n-1},\ \mathbf{Solver}(X^{n-1},\ U^{n-1}(X^{n-1}))).$$
- Time evolution step on *mesh generated by the* $\mathbf{AGR}$ process:
$$(\tilde{X},\ \tilde{U}(\tilde{X})) = \mathbf{AGR}(X^{n-1},\ U^{n-1}(X^{n-1})),$$
$$(X^n,\ U^n(X^n)) = (\tilde{X},\ \mathbf{Solver}(\tilde{X},\ \tilde{U}(\tilde{X}))).$$

3 Numerical Results

Conservative numerical schemes on *non-uniform grids* are applied: Roe's, Lax-Wendroff (LW), MacCormack, MUSCL for scalar conservation laws and for systems of equations with a source term present *well-balanced schemes* are implemented, see [LEV], [HGN], [AD06].

3.1 Burger's with shock waves collision

We first consider numerical experiments for the Burgers equation in the inviscid limit $u_t + \left(u^2/2\right)_x = 0$, with initial conditions given by

$$u(x,0) = \begin{cases} 1.0, & x \in [0.2, 2.0], \\ -0.5, & x \in (2.0, 3.0], \\ -1.0, & x \in (3.0, 4.8], \\ 0.0, & \text{otheriwise.} \end{cases} \tag{2}$$

Numerical results are presented in Fig. 4 at $t = 2s$ when the two shocks have combined into a single one. A grid of 121 points was used for all schemes with CFL number equal to 0.9. All the schemes produce improved results when the adaptive mechanism is imposed, when compared to those produced in a uniform mesh. It is impressive that even the second order oscillatory LW and MacCormack schemes are now able to produce accurate solutions.

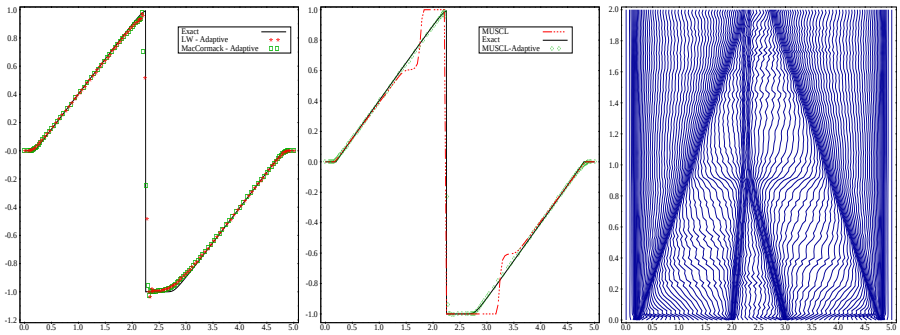

Fig. 4. Numerical solutions and grid point trajectories for the Burgers example

3.2 The shallow water model

The one-dimensional shallow water (SW) system, with a geometrical source term (the bottom topography) added is given as

$$\begin{bmatrix} h \\ hu \end{bmatrix}_t + \begin{bmatrix} hu \\ hu^2 + \frac{g}{2}h^2 \end{bmatrix}_x = \begin{bmatrix} 0 \\ -ghZ_x \end{bmatrix}.$$

where $h(x,t) \geq 0$ is the total water height above the bottom, $u(x,t)$ is the average horizontal velocity, $Z(x)$ is the topography function g the gravitational constant and we denote $q = uh$ the unit discharge.

Idealized Dam-Break Flow. We consider the dam-break problem in a rectangular channel with flat bottom, $Z = 0$. We computed the solution on a channel of length $L = 2000m$ for time $t = 50s$ and with initial conditions:

$$u(x,0) = 0, \qquad h(x,0) = \begin{cases} h_1, & x \leq 1000, \\ h_0, & x > 1000. \end{cases}$$

The results are presented in Figs 6 and 7, with a comparative performance, for various schemes and parameters used, in Table 1.

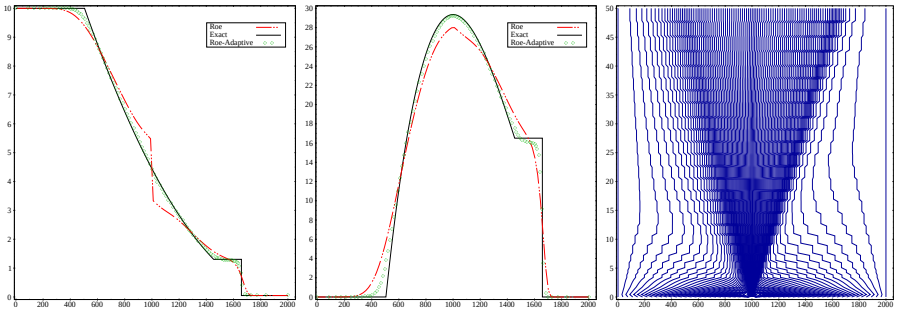

Fig. 5. Idealized Dam-Break: results with Roe's scheme for h (left), q (middle) and grid point trajectories (right) for the adaptive Roe scheme ($p = 0.0518, D = 0.0065$).

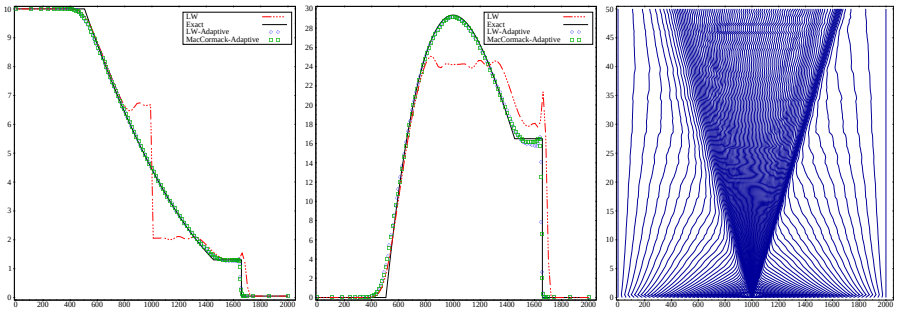

Fig. 6. Numerical solutions for h and $q = uh$ and grid trajectories

Steady transcritical flow with shock over topography. We test the schemes with the adaptive mechanism, in order to study their behavior, to this benchmark problem, [ARV06], with $Z(x)$ given by

$$Z(x) = \begin{cases} 0.2 - 0.05(x-10)^2, & 8 \leq x \leq 12, \\ 0, & \text{otherwise}, \end{cases} \tag{3}$$

in a channel of length $L = 25m$ and an upstream boundary condition for $q = 0.18m^2/s$ and the downstream boundary condition for the water level was $H = 0.33m$. Results are presented in Fig. 7.

Table 1. Idealized Dam-Break: comparative performance

Description	CPU time (sec)	NT	L^1 error (h)	L^1 error (q)
Roe Fixed grid:				
N=101	0.0206	43	0.0113	0.0240
N=201	0.0828	87	0.0077	0.0169
N=401	0.3401	178	0.0049	0.0102
Roe + AGR:				
N= 51, p=0.0500, D= 0.0065	0.0234	77	0.0091	0.0238
N=101, p=0.0500, D= 0	0.1072	178	0.0061	0.0176
N=101, p=0.0500, D= 0.0065	0.0931	158	0.0049	0.0137
TVD Fixed grid:				
N=101	0.0450	44	0.0028	0.0078
N=201	0.1837	90	0.0009	0.0025
N=401	0.7432	180	0.0007	0.0020
TVD + AGR:				
N= 51, p=0.1, D=0.0125	0.0788	136	0.0029	0.0076
N=101, p= 0.1, D=0	0.4292	369	0.0018	0.0055
N=101, p= 0.1, D=0.0125	0.3927	342	0.0007	0.0023

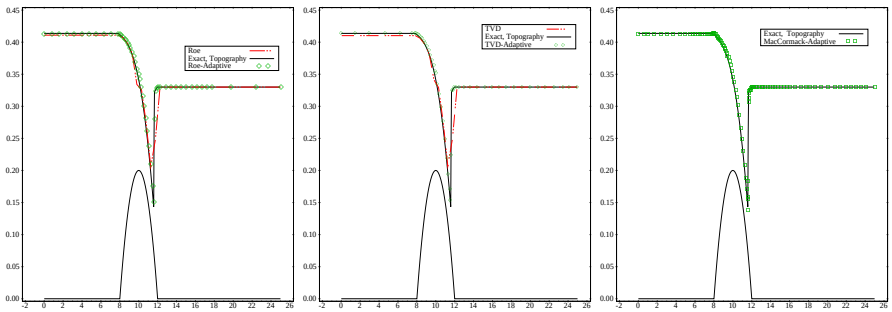

Fig. 7. Numerical solutions for $h + Z$

Dam-Break flow over topography. Here we solve the SW equations with a wavy bottom $Z(x)$

$$Z(x) = \begin{cases} 0.3(\cos(\pi(x-1)/2))^{30}, & |x-1| \leq 1, \\ 0, & \text{otherwise.} \end{cases} \tag{4}$$

and initial conditions

$$h(x,0) = \begin{cases} 2.0 - Z(x), & -10 \leq x < 1, \\ .35 - Z(x), & 1 \leq x < 10, \end{cases} \qquad u(x,0) = \begin{cases} 1, & -10 \leq x < 1, \\ 0, & 1 \leq x < 10, \end{cases} \tag{5}$$

Results are presented in Fig. 8 for the MacCormack scheme (with $p = 0.0345,\ D = 0.001$ at $t = 1s$.

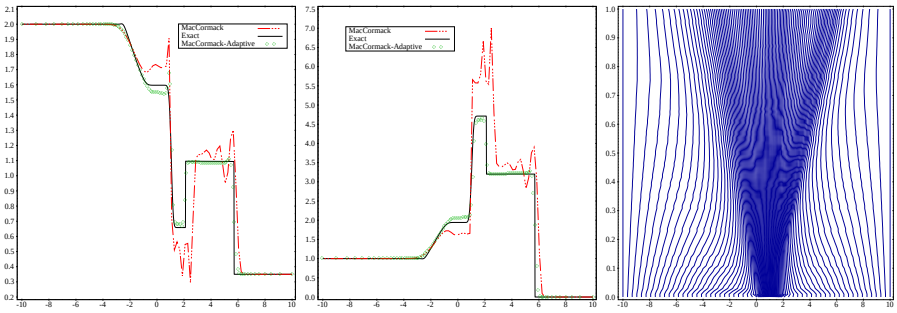

Fig. 8. Numerical solutions for $h + Z$ and $q = uh$ and grid trajectories

4 Conclusions

The **AGR** method proposed here, when applied to classical second order schemes suppresses the oscillations producing *TVD–like* approximations. Classical schemes like the Lax-Wendroff or the Mac-Cormack scheme become stable and can produce reliable solutions. Applied to schemes that do not satisfy entropy conditions, the method approximates the unique entropy solution. The method works well for problems with source terms and produces stable and improved solutions for first and second order balanced schemes. The method can automatically detect, resolve and track steep wave fronts and discontinuities, without having to resort to finer grids. The **AGR** is of linear complexity and its computational cost is in favor when compared, for example, to the stabilization mechanisms for high resolution TVD schemes.

References

[AKM] Arvanitis Ch., Katsaounis Th., and Makridakis Ch.: Adaptive finite element relaxation schemes for hyperbolic conservations laws. M2AN, **35**, 17–33, 2001.

[AMT] Arvanitis Ch., Makridakis Ch. and Tzavaras A.: Stability and convergence of a class of finite element schemes for hyperbolic systems of conservation laws. SIAM J. Numer. Anal., **42**, 1357–1393,2004.

[ARV06] Arvanitis Ch.: Mesh Redistribution Strategies and Finite Element Schemes for Hyperbolic Conservation Laws, (submitted), 2006.

[AD06] Arvanitis Ch. and Delis A.I.: Behavior of Finite Volume Schemes for Hyperbolic Conservation Laws on Adaptive Redistributed Spatial Grids. To appear in SIAM J. on Scientific Computing.

[HGN] Hubbard ME, Garcia-Navarro P.: Flux Difference Splitting and the Balancing of Source terms and Flux Gradients. J. Comp. Phys. 2000; **165**, 89–125, 2000.

[LEV] LeVêque RJ.: Finite Volume Methods for Hyperbolic Problems, Cambridge University Press, 2002.

[TT] Tang H. andTang T.: Adaptive mesh methods for one and two dimensional hyperbolic conservation laws. SIAM J. Numer. Anal., **41**: 487–515, 2003.